THE JOURNAL OF BIOLOGICAL CHEMISTRY VOL. 286, NO. 42, pp. 36667–36676, October 21, 2011
© 2011 by The American Society for Biochemistry and Molecular Biology, Inc. Printed in the U.S.A.

Interaction of Nectin-like Molecule 2 with Integrin $\alpha_6\beta_4$ and Inhibition of Disassembly of Integrin $\alpha_6\beta_4$ from Hemidesmosomes*

Received for publication, November 3, 2010, and in revised form, August 7, 2011 Published, JBC Papers in Press, August 31, 2011, DOI 10.1074/jbc.M110.200535

Kiyohito Mizutani, Satoshi Kawano[1], Akihiro Minami, Masazumi Waseda, Wataru Ikeda[2], and Yoshimi Takai[3]

From the Division of Molecular and Cellular Biology, Department of Biochemistry, and Molecular Biology, Kobe University Graduate School of Medicine, Kobe 650-0017, Hyogo, Japan

In normal epithelial cells, integrin $\alpha_6\beta_4$ is abundantly expressed and forms hemidesmosomes, which is a cellular structure that mediates cell-extracellular matrix binding. In many types of cancer cells, integrin $\alpha_6\beta_4$ is up-regulated, laminin is cleaved, and hemidesmosomes are disrupted, eventually causing an enhancement of cancer cell movement and facilitation of their invasion. We previously showed that the immunoglobulin-like cell adhesion molecule Necl-2 (Nectin-like molecule 2), known as a tumor suppressor, inhibits cancer cell movement by suppressing the ErbB3/ErbB2 signaling. We show here that Necl-2 interacts in *cis* with integrin $\alpha_6\beta_4$. The binding of Necl-2 with integrin β_4 was mediated by its extracellular region. In human colorectal adenocarcinoma Caco-2 cells, integrin $\alpha_6\beta_4$ was localized at hemidesmosomes. Small interfering RNA-mediated suppression of Necl-2 expression enhanced the phorbol ester-induced disruption of the integrin $\alpha_6\beta_4$ complex at hemidesmosomes, whereas expression of Necl-2 suppressed the disruption of this structure. These results indicate that tumor-suppressive functions of Necl-2 are mediated by the stabilization of the hemidesmosome structure in addition to the inhibition of the ErbB3/ErbB2 signaling.

Necl-2 (nectin-like molecule 2) is an Ig-like cell-cell adhesion molecule, which belongs to the Necl family (1). Necl-2 is abundantly expressed in epithelial tissue (2, 3), is undetectable in fibroblasts, such as NIH3T3, Swiss3T3, and L cells (3) and is down-regulated in many types of cancer cells due to hypermethylation of the *Necl-2* gene promoter and/or loss of heterozygosity at chromosome 11q23.2 (2). The Necl family consists of five members, Necl-1, -2, -3, -4, and -5, and comprises a superfamily with the nectin family, which consists of four members, nectin-1, -2, -3, and -4. All members of this superfamily have similar domain structures: one extracellular region with three Ig-like loops, one transmembrane segment, and one cytoplasmic region. Necl-2 has many nomenclatures: IgSF4a, RA175, SgIGSF, TSLC1, SynCAM, and CADM1 (4–8). Necl-2 was originally deposited to GenBank™ in 1998; *IgSF4a* was identified as a candidate for a tumor suppressor gene in the loss of heterozygosity region of chromosome at 11q23.2 (4); *RA175* was identified as a gene highly expressed during neuronal differentiation of embryonic carcinoma cells (7); *SgIGSF* was identified as a gene expressed in spermatogenic cells during earlier stages of spermatogenesis (6); *TSLC1* was identified as a tumor suppressor in human non-small cell lung cancer (5); and SynCAM1 was identified as a brain-specific synaptic adhesion molecule (8). In this study, we use the "Necl-2" because this nomenclature was first reported.

Necl-2 shows Ca^{2+}-independent homophilic cell-cell adhesion activity and Ca^{2+}-independent heterophilic cell-cell adhesion activity with other members of the nectin and Necl families, Necl-1 and nectin-3, and Class-I-restricted T-cell-associated molecule (3, 9, 10). These cell-cell adhesion activities were mediated by their extracellular regions. A cytoplasmic region of Necl-2 is responsible for binding with many peripheral membranous proteins. In particular, the juxtamembrane region of the cytoplasmic region has a band 4.1-binding motif and binds tumor suppressor, DAL-1, the band 4.1 family member, which connects Necl-2 to the actin cytoskeleton (11). In addition, the cytoplasmic region has the PDZ-binding motif at its C-terminal region and binds Pals2, Dlg3/MPP3, and CASK, which are the MAGuK subfamily members that have the L27 domain (3, 8, 12, 13). However, the exact roles of the binding of Necl-2 to these molecules remain unknown.

Necl-2 has been shown to be a tumor suppressor in human non-small cell lung cancer (5), and our previous results indicate that Necl-2 serves as a tumor suppressor by inhibiting the ErbB3/ErbB2 signaling (14). ErbB2 and ErbB3 have kinase domains in their cytoplasmic regions, but that of ErbB3 lacks kinase activity. Therefore, the homo-dimer of ErbB3 formed by binding of heregulin does not transduce any intracellular signaling. By contrast, ErbB2 heterophilically interacts in *cis* with heregulin-occupied ErbB3 and phosphorylates nine tyrosine residues of ErbB3, causing recruitment and activation of the p85 subunit of phosphoinositide 3-kinase and the subsequent activation of Rac small G protein and Akt protein kinase (15). Necl-2 interacts in *cis* with ErbB3, but not with ErbB2, through their extracellular regions and inhibits the heregulin-induced, ErbB2-catalyzed tyrosine phosphorylation of ErbB3 and ErbB3-mediated activation of Rac and Akt, resulting in the inhibition

* This work was supported by the Global COE Program "Global Center for Education and Research in Integrative Membrane Biology" and the Targeted Proteins Research Program from the Ministry of Education, Culture, Sports, Science, and Technology in Japan and by grants-in-aid from the Japan Society for the Promotion of Science.

[1] Present address: Oncology PCU, Eisai Co., Ltd., Tsukuba 300-2635, Ibaraki, Japan.

[2] Present address: KAN Research Institute, Inc., Kobe 650-0047, Hyogo, Japan.

[3] To whom correspondence should be addressed: Div. of Molecular and Cellular Biology, Dept. of Biochemistry and Molecular Biology, Kobe University Graduate School of Medicine, Kobe, 650-0017, Hyogo, Japan. Tel.: 81-78-382-5400; Fax: 81-78-382-5419; E-mail: ytakai@med.kobe-u.ac.jp.

of cancer cell movement and survival. These inhibitory effects of Necl-2 require both the extracellular and cytoplasmic regions and the binding of the cytoplasmic region with protein tyrosine phosphatase PTPN13, also known as a tumor suppressor (14).

Integrin $\alpha_6\beta_4$ is abundantly expressed in normal epithelial cells and forms hemidesmosomes, one of the cell-extracellular matrix (ECM)[4] junctions (16). Hemidesmosomes are classified into two types: types I and II. Type I is mainly observed in keratinocytes in the skin, whereas type II is in intestinal epithelial cells. It was also reported that integrin $\alpha_6\beta_4$ physically and functionally interacts with ErbB2, causing the enhancement of ErbB2 signaling for cell proliferation and motility (17–19). Furthermore, our recent finding suggests that ErbB3, but not ErbB2, interacts in *cis* with integrin $\alpha_6\beta_4$, implicating heregulin-induced ErbB3/ErbB2-mediated DNA synthesis (20). Hemidesmosomes play roles in keeping epithelial cell morphology and inhibiting cell movement. The extracellular region of integrin $\alpha_6\beta_4$ preferentially binds to laminin-332, a major component of epithelial basement membrane, whereas the cytoplasmic region of integrin β_4 directly interacts with plectin and associates with keratin intermediate filaments. The formation of hemidesmosomes by laminin-332 and integrin $\alpha_6\beta_4$ mediates stable cell-ECM anchorage, which enables the cells to resist mechanical stresses (21). In many types of cancer cells, integrin $\alpha_6\beta_4$ is up-regulated, laminin is cleaved, and hemidesmosomes are disrupted, eventually causing an enhancement of cancer cell movement and a facilitation of their invasion (22). Here, we report that Necl-2 interacts in *cis* with integrin $\alpha_6\beta_4$ and inhibits the disassembly of integrin $\alpha_6\beta_4$ from hemidesmosomes.

EXPERIMENTAL PROCEDURES

Constructions—FLAG-tagged Necl-1 expression vector (pCAGIPuro-FLAG-Necl-1) was prepared as described (3). FLAG-tagged Necl-2, Necl-3, and Necl-4 expression vectors (pCAGIPuro-FLAG-Necl2, pCAGIPuro-FLAG-Necl-3, pCAGIPuro-FLAG-Necl-4) were prepared as described (14). FLAG-tagged Necl-5 expression vector was prepared as described (23). The plasmids pCAGIPuro-FLAG-Necl-2-ΔCP and pCAGIPuro-FLAG-Necl-2-ΔEC were described previously (14). The following expression vectors were kindly provided: integrin α_6 and integrin β_4 from Dr. A. Sonnenberg (The Netherlands Cancer Institute, Amsterdam, The Netherlands) and integrin α_5 and integrin β_1 from Dr. J. C. Norman (Beatson Institute for Cancer Research, Glasgow, Scotland, UK).

Antibodies and Reagents—A rabbit anti-Necl-2 polyclonal antibody was prepared as described previously (14). The following rabbit polyclonal antibodies were purchased from commercial sources: anti-FLAG (for Western blotting, Sigma-Aldrich), anti-integrin β_4 (clone H-101 for Western blotting, Santa Cruz Biotechnology), and anti-integrin β_1 (Millipore). The following mouse mAbs were purchased from commercial sources: anti-FLAG M2 (for immunoprecipitation, Sigma-Aldrich), anti-integrin β_4 (for immunostaining, BD Biosciences; for immunoprecipitation, Millipore), and anti-actin (Millipore). A rat mAb for integrin α_6 was purchased from Progen. Fluorophore-conjugated secondary Abs were purchased from Jackson ImmunoResearch Laboratories. Horseradish peroxidase-conjugated secondary Abs and protein G-Sepharose 4 Fast Flow were purchased from GE Healthcare. Fatty acid-free BSA, a trypsin inhibitor, phosphatase inhibitor mixture, and 12-*O*-tetradecanoylphorbol-13-acetate (TPA) were purchased from Sigma-Aldrich. Growth factor-reduced Matrigel matrix without phenol red was purchased from BD Biosciences. Recombinant human laminin-332 was obtained from Oriental Yeast Company (Tokyo, Japan). pAcGFP1-Mem plasmid was purchased from Clontech.

Cell Culture—Caco-2 cells were purchased from the European Collection of Cell Cultures and maintained in DMEM supplemented with 10% fetal calf serum and 0.1 mM non-essential amino acids. HEK293 cells were maintained in DMEM supplemented with 10% fetal calf serum. All cells were maintained in culture at 37 °C in a humidified 5% CO_2 incubator.

Co-immunoprecipitation Assay—HEK293 cells were co-transfected with various combinations of plasmids using Lipofectamine 2000 reagent (Invitrogen), according to the manufacture's protocol. HEK293 cells cultured for 48 h were detached with 0.05% trypsin and 0.53 mM EDTA, and then treated with a trypsin inhibitor. Cells were cultured in suspension with DMEM containing 0.5% fatty acid-free BSA for 30 min, collected by centrifugation, washed with wash buffer (20 mM Tris-HCl, pH 8.0, 150 mM NaCl, and 1 mM Na_3VO_4), and lysed with lysis buffer (20 mM Tris-HCl, pH 8.0, 150 mM NaCl, 1 mM $CaCl_2$, 1 mM $MgCl_2$, 10% glycerol, 1% Nonidet P-40, 10 mM NaF, 1 mM Na_3VO_4, 10 μg/ml leupeptin, 2 μg/ml aprotinin, 10 mM (*p*-amidinophenyl)methanesulfonyl fluoride, and phosphatase inhibitor mixture I). The lysates were rotated at 4 °C for 30 min and subjected to centrifugation at 12,000 × *g* for 15 min. The supernatant was pre-cleared with protein G-Sepharose 4 Fast Flow beads at 4 °C for 1 h. The anti-FLAG M2 mAb was preincubated with protein G-Sepharose beads at 4 °C for 2 h. The cell extracts were incubated with the anti-FLAG M2 mAb-conjugated protein G-Sepharose beads at 4 °C for 4 h. After the beads were extensively washed with the lysis buffer, bound proteins were eluted by boiling the beads in SDS sample buffer (60 mM Tris-HCl, pH 6.7, 3% SDS, 2% 2-mercaptoethanol, and 5% glycerol) for 5 min, and subjected to SDS-PAGE, followed by Western blotting using the indicated Abs.

siRNA Experiments—Stealth RNAi duplexes against human Necl-2 and human integrin β_4 and a stealth RNAi negative control duplex were purchased from Invitrogen. For knockdown of Necl-2, the stealth RNAi duplex of 5′-GGUGAGGAGAUUGAAGUCAACUGCA-3′ was used. For knockdown of integrin β_4, the stealth RNAi duplex of 5′-UGAACAUCUCGUCUGUGCAGUAGGC-3′ was used. Transfection of cells with siRNA was performed using Lipofectamine RNAiMAX reagent (Invitrogen) according to the manufacturer's instructions.

Cell Adhesion Assay—Cell adhesion assay was performed as described with a slight modification (24). Briefly, 96-well plates were coated at 4 °C overnight with laminin-332 or Matrigel and blocked with 1% BSA in PBS for 30 min at room temperature. Cells were harvested by treating with 0.53 mM

[4] The abbreviations used are: ECM, extracellular matrix; TPA, 12-*O*-tetradecanoylphorbol-13-acetate.

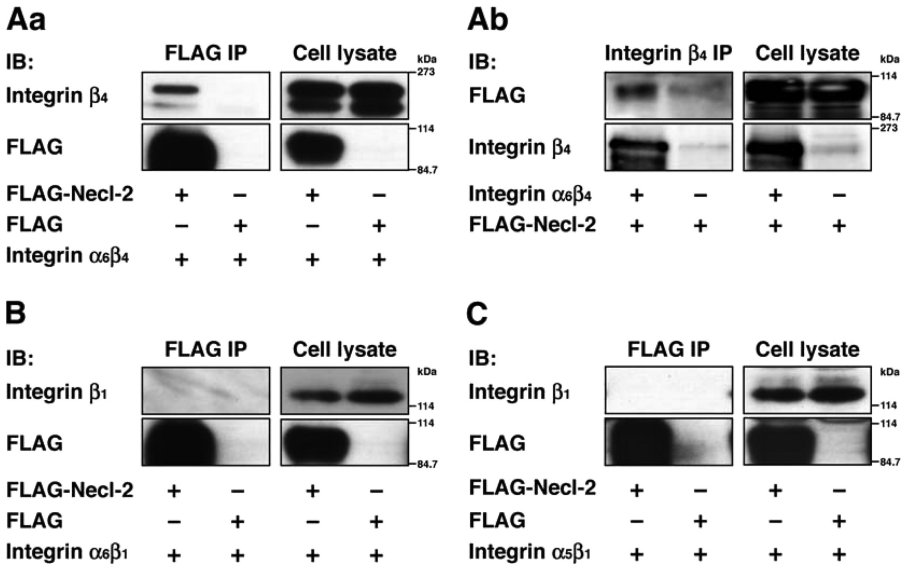

FIGURE 1. **Interaction of Necl-2 with integrin $\alpha_6\beta_4$.** HEK293 cells were co-transfected with various combinations of the indicated plasmids and cultured in suspension. FLAG-tagged Necl-2 was immunoprecipitated using the anti-FLAG mAb (*A*, *panel a*, *B*, and *C*) or integrin β_4 was immunoprecipitated using the anti-integrin β_4-mAb (*A*, *panel b*), and samples were subjected to Western blotting using the indicated Abs. *A*, *panels a and b*, FLAG-Necl-2 and integrin $\alpha_6\beta_4$; *B*, FLAG-Necl-2 and integrin $\alpha_6\beta_1$; *C*, FLAG-Necl-2 and integrin $\alpha_5\beta_1$. *IB*, immunoblot.

EDTA in PBS and were collected by centrifugation. The collected cells were rinsed in an ice-cold adhesion buffer (DMEM containing 15 mM HEPES and 0.2% BSA). After washing with the adhesion buffer, the cells were plated at a density of 5×10^4 cells per well and incubated at 37 °C for 1 h. The cells attached to the dish were fixed with 4% paraformaldehyde and stained with 0.2% crystal violet in 1% ethanol solution. After extensive washing in water, the plates were dried overnight. Crystal violet was extracted by incubating the plates with 0.1 M sodium citrate in 50% ethanol for 15 min, after which absorbance at 595 nm was measured as an indicator of the numbers of cells attached.

Immunofluorescence Microscopy—Cells were seeded onto coverslips coated with a thin layer of Matrigel or onto coverslips coated with laminin-332. For TPA stimulation, the medium was replaced with a fresh medium containing 50 ng/ml TPA. After indicated time periods, the cells were fixed with acetone/methanol (1:1) on ice for 1 min, followed by incubation with 20% BlockAce (Dainippon Sumitomo Pharma) in PBS. The samples were then incubated with primary Abs, followed by incubation with appropriate fluorophore-conjugated secondary Abs. The samples were then washed three times with PBS and mounted in Prolong Gold mount gel (Invitrogen). Fluorescence signals were visualized by a confocal laser scanning microscopy (Digital Eclipse C1si-ready, Nikon).

RESULTS

Interaction of Necl-2 in Cis with Integrin β_4—Epithelial cells abundantly express integrin $\alpha_6\beta_4$, $\alpha_5\beta_1$, and $\alpha_6\beta_1$ (25, 26). We first examined whether Necl-2 interacts with these integrins. FLAG-tagged Necl-2 (FLAG-Necl-2) or FLAG alone together with integrin $\alpha_6\beta_4$, $\alpha_5\beta_1$, or $\alpha_6\beta_1$ were co-expressed in HEK293 cells, and the cells were cultured in suspension. The suspension culture of HEK293 cells enabled the detection of a possible *cis*-interaction between Necl-2 and integrins on the plasma membrane. When FLAG-Necl-2 was immunoprecipitated from each cell lysate using the anti-FLAG mAb, integrin $\alpha_6\beta_4$ was co-immunoprecipitated (Fig. 1*A*, *panel a*). When integrin β_4 was precipitated from the lysates of HEK293 cells expressing integrin $\alpha_6\beta_4$ and FLAG-Necl-2, FLAG-Necl-2 was co-immunoprecipitated (Fig. 1*A*, *panel b*). Integrin $\alpha_5\beta_1$ or $\alpha_6\beta_1$ was not co-immunoprecipitated with FLAG-Necl-2 (Fig. 1, *B* and *C*). These results indicate that Necl-2 specifically interacts in *cis* with integrin $\alpha_6\beta_4$.

We then examined whether the extracellular region and/or the cytoplasmic region of Necl-2 are necessary for the interaction with integrin $\alpha_6\beta_4$. The mutants of FLAG-Necl-2 in which the cytoplasmic region or the extracellular region was deleted (FLAG-Necl-2-ΔCP or FLAG-Necl-2-ΔEC, respectively) and integrin $\alpha_6\beta_4$ were co-expressed in HEK293 cells. Integrin $\alpha_6\beta_4$ was co-immunoprecipitated with FLAG-Necl-2-ΔCP, but not with FLAG-Necl-2-ΔEC (Fig. 2, *A* and *B*). The amount of integrin $\alpha_6\beta_4$ that was co-immunoprecipitated with FLAG-Necl-2-ΔCP was about four times as much as that co-immunoprecipitated with the full-length FLAG-Necl-2 (Fig. 2*B*). These results indicate that Necl-2 interacts in *cis* with integrin $\alpha_6\beta_4$ through its extracellular region and that the cytoplasmic region may have an inhibitory effect for the interaction of the extracellular region of Necl-2 with integrin $\alpha_6\beta_4$.

Necl-2 is a member of the Necl family, which consists of five members. We therefore examined whether other members of Necl family proteins also interact with integrin $\alpha_6\beta_4$. FLAG-tagged members of this family were co-expressed with integrin $\alpha_6\beta_4$ in HEK293 cells, and a similar co-immunoprecipitation assay was performed. Integrin $\alpha_6\beta_4$ was co-immunoprecipitated with FLAG-Necl-1 and -4 in addition to FLAG-Necl-2 (Fig. 3*A*). Integrin $\alpha_6\beta_4$ was also co-immunoprecipitated with FLAG-Necl-3 and -5, but to lesser extents than with Necl-1, -2, and -4 (Fig. 3*B*). These results indicate that integrin $\alpha_6\beta_4$ interacts broadly with the members of the Necl family.

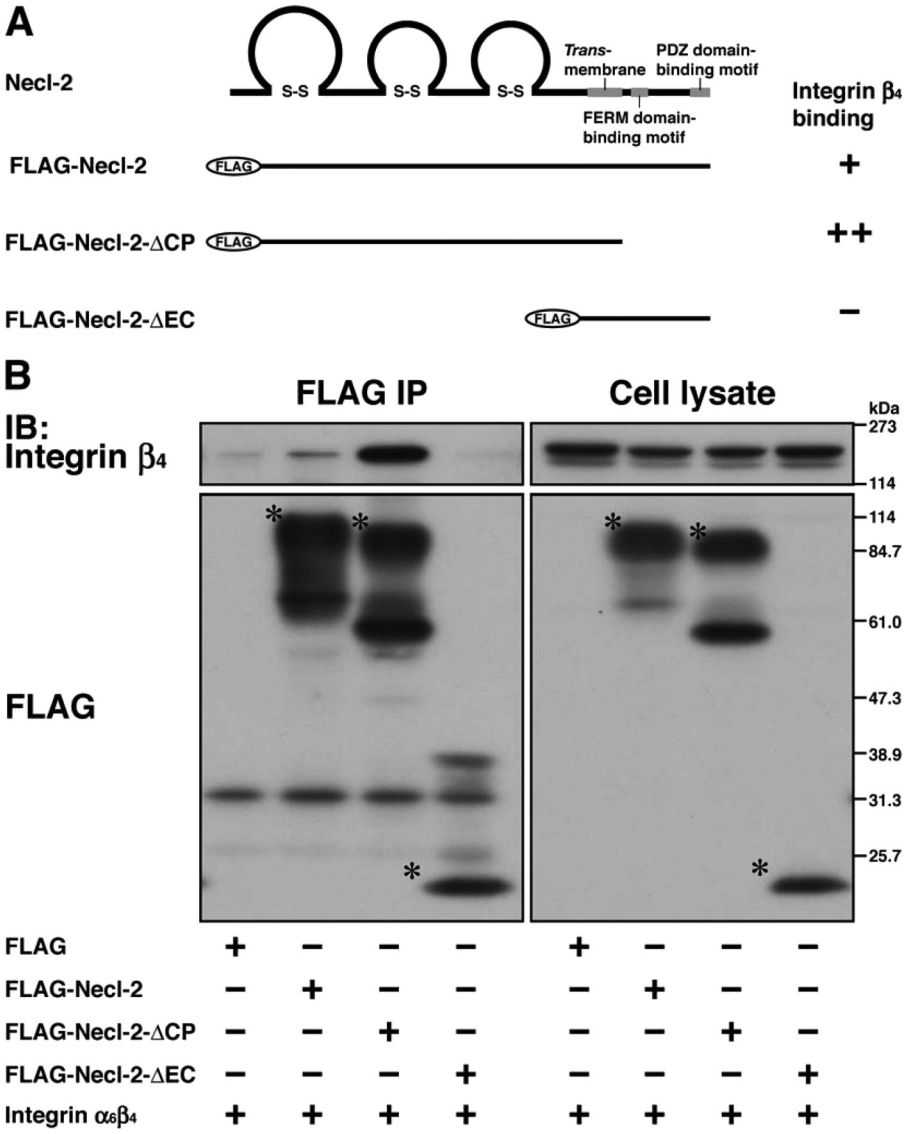

FIGURE 2. **Interaction of Necl-2 with integrin $\alpha_6\beta_4$ through its extracellular region.** *A*, schematic diagram of Necl-2 fragments. Necl-2 fragments were tagged with a FLAG epitope at the N terminus. *FERM*, 4.1/ezrin/radixin/moesin. +, positive for the interaction with integrin β_4; −, negative for the interaction with integrin β_4. *B*, HEK293 cells were co-transfected with various combinations of the indicated plasmids and cultured in suspension. FLAG-tagged full-length Necl-2 or deletion mutants of Necl-2 were immunoprecipitated using the anti-FLAG-mAb, and samples were subjected to Western blotting using the indicated Abs. *Asterisks*, full-length or mutants of Necl-2. *IB*, immunoblot.

Localization of Integrin $\alpha_6\beta_4$ at Hemidesmosome-like Structure in Caco-2 Cells—To clarify subcellular localization of integrin $\alpha_6\beta_4$, we stained human adenocarcinoma Caco-2 epithelial cells cultured on Matrigel using specific Abs against integrin α_6 and integrin β_4 and analyzed by a confocal microscopy. The streaky immunofluorescence signals for integrin α_6 and integrin β_4 were observed at the cell-ECM adhesion levels in Caco-2 cells (Fig. 4*A*). This signal for integrin α_6 disappeared when integrin β_4 was knocked down by its siRNA (Fig. 4*B*). Marked reduction of integrin β_4 protein expression was confirmed by Western blotting (Fig. 4*C*). These results indicate that the integrin $\alpha_6\beta_4$-dependent structure most likely corresponds to hemidesmosomes in Caco-2 cells.

Co-localization of Necl-2 and Integrin β_4 at Basal Side of Lateral Plasma Membrane—To confirm that Necl-2 and integrin $\alpha_6\beta_4$ are in a common complex in Caco-2 cells cultured on Matrigel, we stained the cells using the Abs against Necl-2 and integrin β_4. The immunofluorescence signal for Necl-2 was predominantly concentrated at the lateral plasma membrane of the cells (Fig. 5). The signal for integrin β_4 was concentrated both at the hemidesmosome-like structure of the cell-ECM adhesion site and at the basal side of the lateral plasma membrane, where the signal for integrin β_4 was partly overlapped with that for Necl-2 (Fig. 5). These results, together with the results presented above (Figs. 1–3), indicate that Necl-2 and integrin $\alpha_6\beta_4$ are at least in part in a common complex in Caco-2 cells.

Regulation by Necl-2 of TPA-induced Disassembly of Hemidesmosome-like Structure—The tumor-promoting phorbol ester TPA was shown to induce the disassembly of integrin $\alpha_6\beta_4$ from hemidesmosomes in A431 cells (27). We observed that the hemidesmosome-like structure visualized by the anti-integrin α_6 antibody were disappeared when Caco-2 cells cultured on Matrigel were incubated with TPA, indicat-

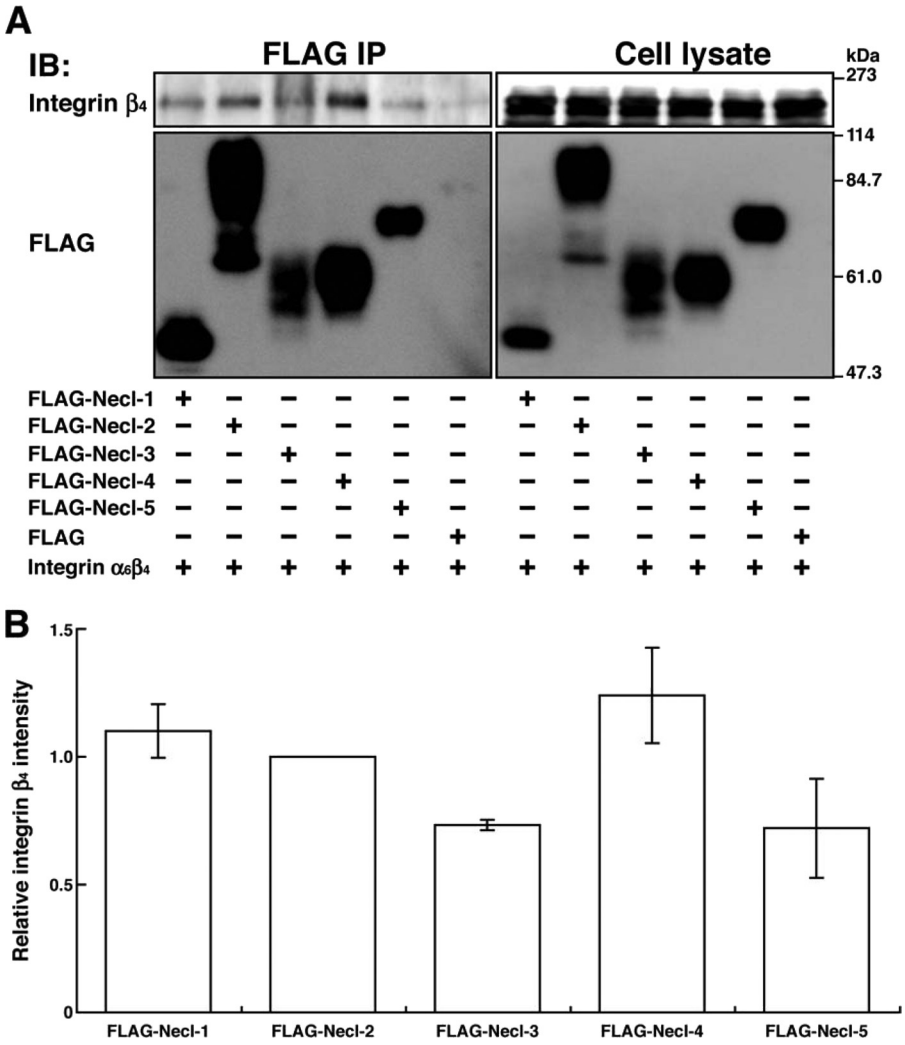

FIGURE 3. **Interaction of integrin $\alpha_6\beta_4$ with Necl family proteins.** *A*, HEK293 cells were co-transfected with various combinations of the indicated plasmids and cultured in suspension. Each FLAG-tagged Necl family protein was immunoprecipitated using the anti-FLAG mAb, and samples were subjected to Western blotting using the indicated Abs. *B*, the band intensity of immunoprecipitated integrin β_4 was first normalized against that of immunoprecipitated Necl family members, and then the relative values were represented in the graph by setting a value of the Necl-2-immunoprecipitated integrin β_4 as 1. *Error bars* indicated the means ± S.E. of three independent experiments. *IB*, immunoblot.

ing that TPA induces disassembly of integrin $\alpha_6\beta_4$ from the hemidesmosome-like structure in Caco-2 cells (Fig. 6, *A*, *panel a*, and *B*).

We then examined the effect of Necl-2 on the TPA-induced disruption of the hemidesmosome-like structure in Caco-2 cells. We analyzed a time course of the TPA-induced disruption of the hemidesmosome-like structure. In the absence of TPA, the percentage of the hemidesmosome-positive cells in number were similar among the control, Necl-2 knockdown, and Necl-2-overexpressing Caco-2 cells, suggesting that expression levels of Necl-2 did not affect the formation of the hemidesmosome-like structure. However, Necl-2 knockdown significantly enhanced the TPA-induced disruption of the hemidesmosome-like structure (Fig. 6, *A*, *panel b*, and *B*), whereas overexpression of Necl-2 clearly delayed the disruption process (Fig. 6, *A*, *panel c*, and *B*). The expression level of Necl-2 was decreased in Necl-2 knockdown cells and increased in Necl-2-overexpressing cells (Fig. 6*C*). Taken together, these results indicate that Necl-2 inhibits the disassembly of integrin $\alpha_6\beta_4$ from the hemidesmosome-like structure.

No Effect of Necl-2 on Initial Caco-2 Cell Attachment—To test whether initial integrin-ECM cell attachment ability is altered by the difference of Necl-2 expression levels, we performed a cell adhesion assay by using laminin-332 or Matrigel as an ECM. When the same numbers of wild-type, Necl-2 knockdown, and Necl-2-overexoressing Caco-2 cells were allowed to attach onto laminin-332-coated plates, similar numbers of the cells were attached (Fig. 7). Similar results were obtained when the cells were allowed to attach onto Matrigel-coated plates. Taken together, these results indicate that the expression level of Necl-2 does not affect the initial cell attachment ability.

Inhibitory Effect of Necl-2 on TPA-induced Disassembly of Hemidesmosome-like Structure of Caco-2 Cells Cultured on Laminin-332—To confirm that the Necl-2-dependent inhibitory effect of hemidesmosome disassembly could also be observed with Caco-2 cells cultured on laminin-332, we performed the similar TPA-induced hemidesmosome disassembly experiments using laminin-332 as an ECM. Similar to that observed with Caco-2 cells cultured on Matrigel, Necl-2 knock-

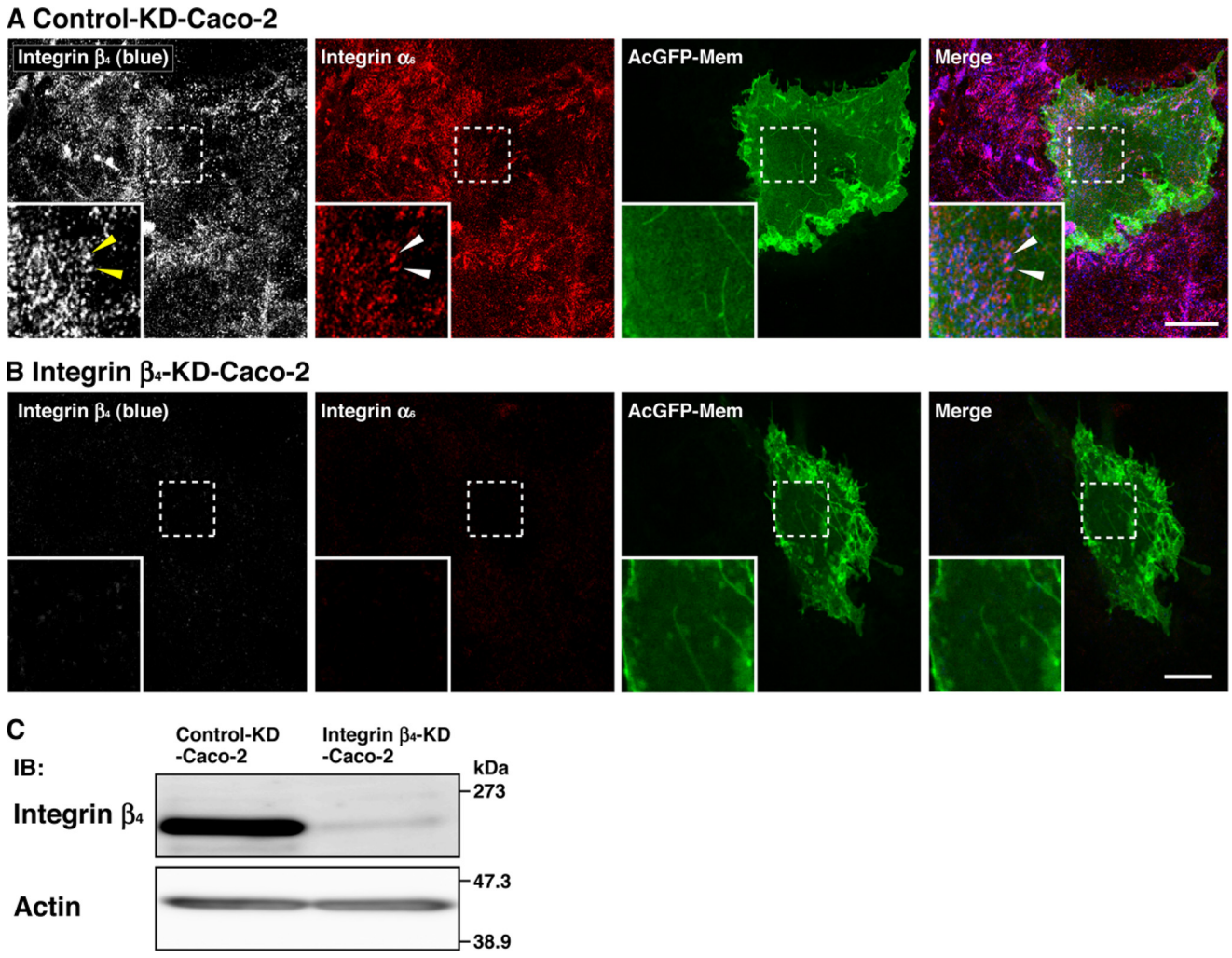

FIGURE 4. **Localization of integrin $\alpha_6\beta_4$ in the hemidesmosome-like structure of Caco-2 cells.** Caco-2 cells were transfected with a stealth RNAi negative control duplex or a stealth RNAi duplex against human integrin β_4. To make the cell border clear, pAcGFP1-Mem vector was co-transfected. Confluent cell monolayers of control (Control-KD-Caco-2) and integrin β_4 knockdown (Integrin β_4-KD-Caco-2) Caco-2 cells were stained with the anti-integrin β_4 and the anti-integrin α_6 Abs. *Inset boxes* show the area of high magnification images. *Scale bars*, 10 μm. *A*, control-KD-Caco-2 cells; *B*, integrin β_4-KD-Caco-2 cells. *Arrowheads*, hemidesmosome-like structure. *C*, expression level of integrin β_4 in control-KD-Caco-2 and integrin-β_4-KD-Caco-2 cells. Lysates from control-KD-Caco-2 and integrin-β_4-KD-Caco-2 cells were separated by SDS-PAGE, followed by Western blotting using the anti-integrin-β_4 and the anti-actin Abs. *IB*, immunoblot.

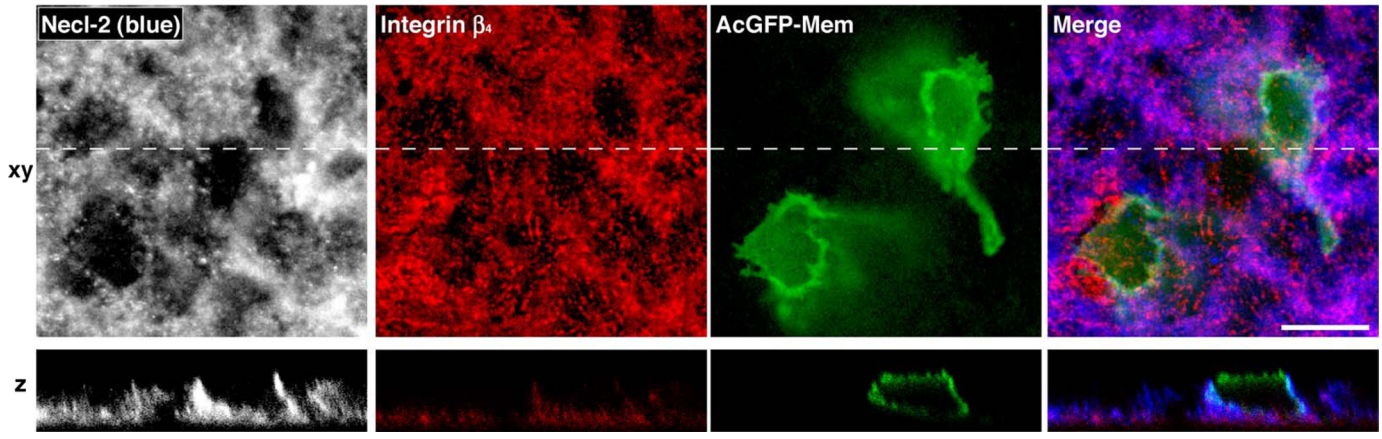

FIGURE 5. **Co-localization of Necl-2 with integrin β_4 at the basal side of the lateral plasma membrane.** Immunofluorescence staining for integrin β_4 and Necl-2 in Caco-2 cells. Caco-2 cells were transfected with pAcGFP1-Mem to make the cell border clear. Confluent monolayers of Caco-2 cells were stained with the anti-integrin β_4 and the anti-Necl-2 Abs. The *dashed lines* in the *xy* sectional images correspond to the sites of the *z* sections. *Scale bar*, 10 μm.

down significantly enhanced the TPA-induced disruption of the hemidesmosome-like structure, whereas overexpression of Necl-2 clearly delayed the disruption process (Fig. 8). These results, together with the results of Fig. 6, indicate that Necl-2 inhibits the disassembly of integrin $\alpha_6\beta_4$ from the hemidesmosome-like structure.

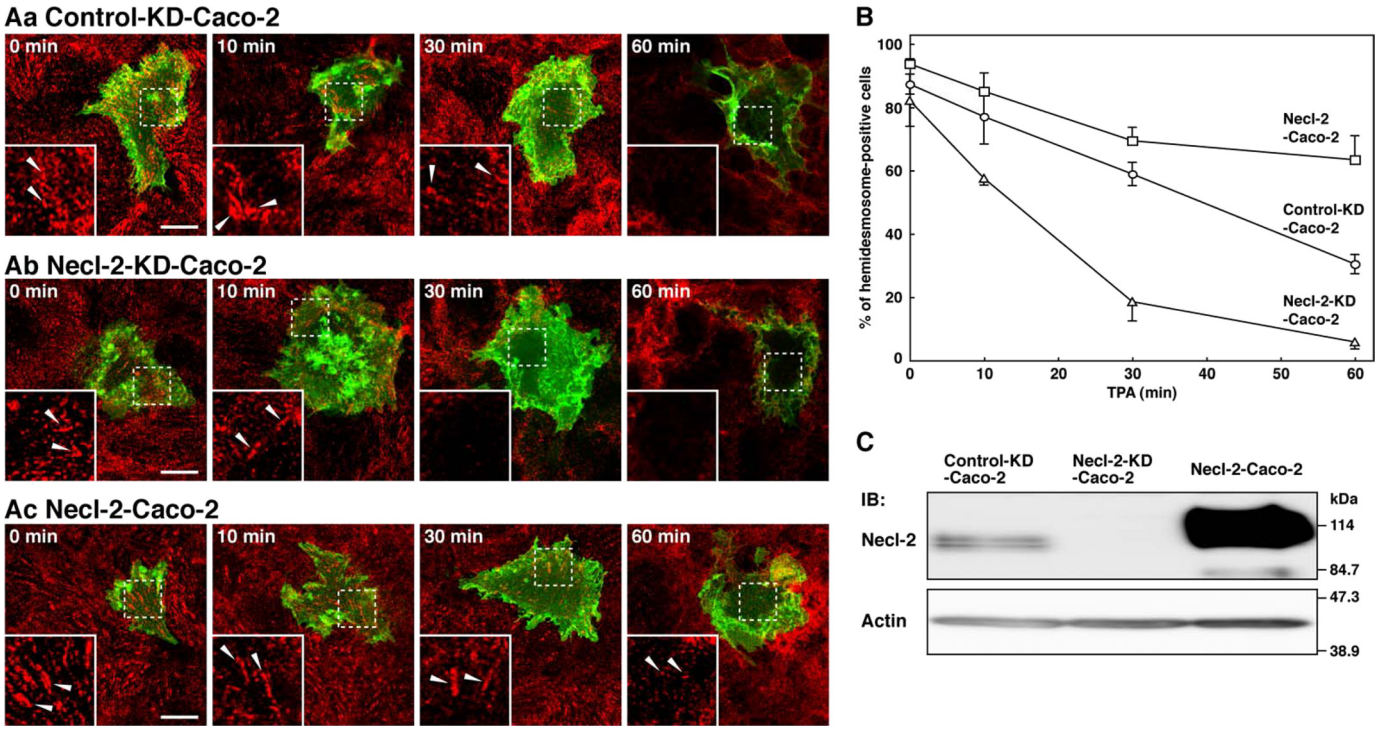

FIGURE 6. **Regulation by Necl-2 of the TPA-induced disassembly of the hemidesmosome-like structure.** *A*, TPA-induced disassembly of the hemidesmosome-like structure. Caco-2 cells were transfected with a stealth RNAi negative control duplex or a stealth RNAi duplex against human Necl-2. To make the cell border clear, pAcGFP1-Mem vector was co-transfected. Confluent Caco-2 cell monolayers of control-knockdown (*A*, *panel a*, control-KD-Caco-2), Necl-2 knockdown (*A*, *panel b*, Necl-2-KD-Caco-2), and Necl-2-overexpressing (*A*, *panel c*, Necl-2-Caco-2) cells were stimulated with TPA (50 ng/ml) for the indicated time periods. The cells were stained with the anti-integrin α_6 Ab. *Inset boxes* show the area of high magnification images. *Scale bars*, 10 μm. *Arrowheads*, hemidesmosome-like structure. *B*, time course of disassembly of the hemidesmosome-like structure. The number of hemidesmosome-like structure positive cells were counted by microscopic examination. *Circles*, control-KD-Caco-2; *triangle*, Necl-2-KD-Caco-2; *squares*, Necl-2-Caco-2. The results are given as the means ± S.D. *C*, expression level of Necl-2 in control-KD-Caco-2, Necl-2-KD-Caco-2, and Necl-2-Caco-2 cells. Lysates from indicated cells were separated by SDS-PAGE, followed by Western blotting using the anti-Necl-2 and anti-actin Abs. *IB*, immunoblot.

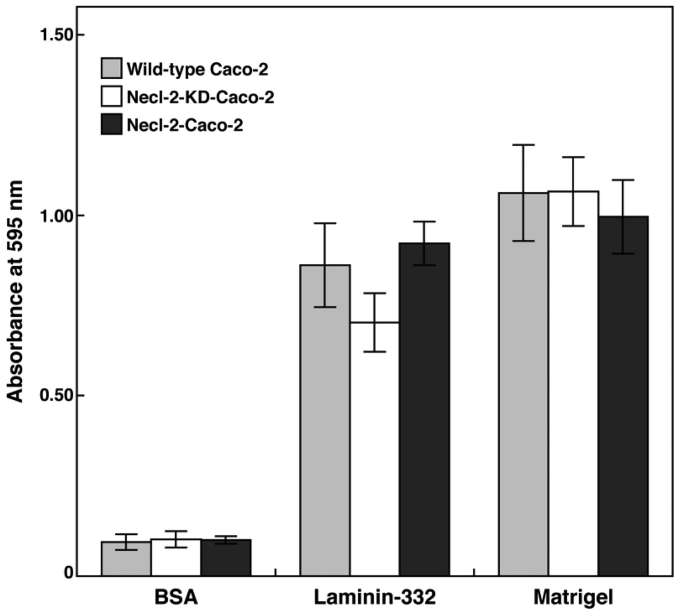

FIGURE 7. **No effect of Necl-2 on initial Caco-2 cell attachment.** Wild-type Caco-2 cells, Necl-2 knockdown Caco-2 cells (Necl-2-KD-Caco-2), and Necl-2-overexpressing Caco-2 cells (Necl-2-Caco-2) were plated onto plates coated with BSA, laminin-332, and Matrigel. Cells were allowed to attach at 37 °C for 1 h, non-attached cells were removed, and the cells were subjected to fixation. The fixed cells were stained with crystal violet. Dye was extracted by 0.1 M sodium citrate in 50% ethanol for 15 min, and absorbance at 595 nm was measured as an indicator of the numbers of the attached cells. The results are given as the means ± S.D.

DISCUSSION

We previously showed that Necl-2 interacts in *cis* with ErbB3, but not with ErbB2, and inhibits the heregulin-induced activation of the ErbB3/ErbB2 signaling (14). In addition, we showed that ErbB3, but not ErbB2, interacts in *cis* with integrin $\alpha_6\beta_4$, although it had been shown that ErbB2 interacts with integrin $\alpha_6\beta_4$ (20). We showed here that Necl-2 interacts with integrin $\alpha_6\beta_4$. These two molecules is likely to interact with each other in *cis* because the co-immunoprecipitation assay was performed using suspended HEK293 cells, which did not contact with each other. The interaction of Necl-2 with integrin $\alpha_6\beta_4$ is specific because it does not interact with integrin $\alpha_6\beta_1$ or $\alpha_5\beta_1$. We further showed here that the extracellular region of Necl-2 binds to the extracellular region of integrin $\alpha_6\beta_4$. Although the cytoplasmic region of Necl-2 is not required for this interaction, it may suppress the interaction of the extracellular region of Necl-2 with integrin $\alpha_6\beta_4$ because deletion of the cytoplasmic region strongly increased the affinity of Necl-2 with integrin $\alpha_6\beta_4$.

Each Necl family member consists of ~400 amino acids with a predicted molecular mass of 42.8–48.5 kDa. It was reported that Necl family members show an upward mobility shift by *N*-glycosylation (28). Consistent with these results, transiently expressed Necl family members in HEK293 cells showed similar upward mobility shift (Fig. 3*A*). Therefore, the wide spectrum of recombinant Necl family members is attributable to

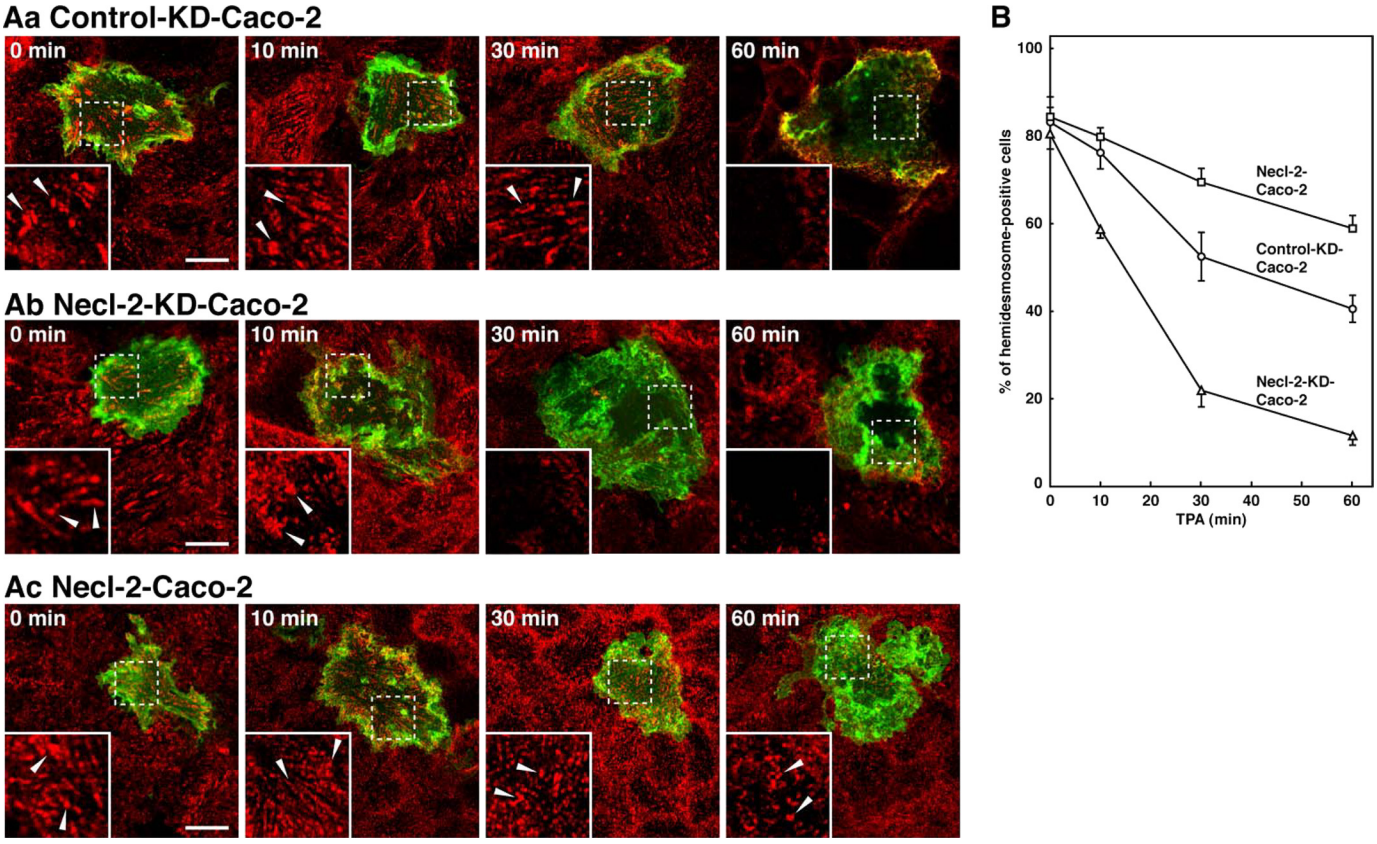

FIGURE 8. **The inhibitory effect of Necl-2 on the TPA-induced disassembly of the hemidesmosome-like structure of Caco-2 cells cultured on laminin-332.** *A*, TPA-induced disassembly of the hemidesmosome-like structure. Caco-2 cells were transfected with a stealth RNAi negative control duplex or a stealth RNAi duplex against human Necl-2. To make the cell border clear, pAcGFP1-Mem vector was co-transfected. Confluent Caco-2 cell monolayers of control-knockdown (*A*, *panel a*, Control-KD-Caco-2), Necl-2 knockdown (*A*, *panel b*, Necl-2-KD-Caco-2), and Necl-2-overexpressing (*A*, *panel c*, Necl-2-Caco-2) cells were stimulated with TPA (50 ng/ml) for indicated time periods. The cells were stained with the anti-integrin α_6 Ab. *Inset boxes* show the area of high magnification images. *Scale bars*, 10 μm. *Arrowheads*, hemidesmosome-like structure. *B*, time course of disassembly of the hemidesmosome-like structure. The number of the hemidesmosome-like structure positive cells was counted by microscopic examination. *Circles*, control-KD-Caco-2; *triangles*, Necl-2-KD-Caco-2; *squares*, Necl-2-Caco-2. The results are given as the means ± S.D.

the difference of *N*-glycosylation between the Necl family members.

Integrin $\alpha_6\beta_4$ is abundantly expressed in normal epithelial cells and forms hemidesmosomes, which play key roles in keeping epithelial cell morphology and inhibiting cell movement (16). In Caco-2 epithelial cells, integrin β_4 is predominantly localized at the cell-matrix adhesion and co-localized with integrin α_6. The signal for integrin α_6 disappeared from the basal region of integrin β_4 knockdown Caco-2 cells, indicating that the integrin $\alpha_6\beta_4$-dependent structure most likely corresponds to hemidesmosomes in Caco-2 cells. We previously showed that the immunogold particles for Necl-2 were concentrated at the basolateral plasma membrane of the epithelial cells of gall bladder (3): Underwood *et al.* (29) showed that integrin β_4 localized not only at the hemidesmosomes but also at the lateral filopodic cell-cell adhesion sites of keratinocytes. Although the tissue types analyzed were different, these results suggest a possibility of the co-localization of Necl-2 with integrin $\alpha_6\beta_4$ *in vivo* and are consistent with our present finding that Necl-2 and integrin $\alpha_6\beta_4$ are at least in part in a common complex in Caco-2 cells.

Not only integrins but also ECMs play important roles in the formation of cell-ECM adhesions, such as hemidesmosomes, focal complexes, and focal adhesions. Matrigel is one of the widely used basement membrane substrate because it was reported that it is composed of laminin as a major component, followed by collagen IV, heparan sulfate proteoglycans, entactin/nidogen, resembling the ECM found in many tissues (30, 31). Among laminins, laminin-332 is a major component of the epithelial basement membrane and a main ligand of integrin $\alpha_6\beta_4$ (21). In the cell adhesion assay, the same numbers of the control, Necl-2 knockdown, and Necl-2-overexpressing cells attached onto laminin-332-coated plates and Matrigel-coated plates. We did not observe any gain or loss of initial cell attachment abilities among these cell types, suggesting that it is unlikely that Necl-2 modifies the initial cell attachment ability.

When Caco-2 cells were stimulated with the tumor-promoting phorbol ester TPA, disassembly of the hemidesmosome-like structure was observed in a time-dependent manner, consistent with an earlier observation in A431 cells (27). Moreover, knockdown of Necl-2 accelerated this hemidesmosome-like structure disassembly, whereas overexpression of Necl-2 delayed the disassembly process. In the absence of TPA, there was no difference in hemidesmosome-positive cell ratio among the control, Necl-2-overexpressing, and Necl-2 knockdown Caco-2 cells, suggesting that Necl-2 specifically plays an important role in the inhibition of the TPA-induced hemidesmosome disassembly. Co-localization of Necl-2 with integrin β_4 was

mainly observed at the basal side of the lateral plasma membrane, indicating that Necl-2 forms a complex with integrin $\alpha_6\beta_4$ at this region and inhibits the TPA-induced hemidesmosome disassembly. We presented the role of Necl-2 in hemidesmosome regulation, but further studies are required to improve our understanding of the underlying mechanism. One possible mechanism predicted at this time is that tumor necrosis factor-α converting enzyme is involved in this process. There are several studies showing that TPA treatment of cells induces tumor necrosis factor-α converting enzyme activation, followed by extracellular domain cleavage of membrane proteins, such as amyloid precursor protein, ErbB4, and nectin-1 (32–35). In addition to these substrates, both Necl-2 and integrin β_4 are also cleaved by tumor necrosis factor-α converting enzyme (36, 37). It is possible that the cleavage of integrin β_4 by tumor necrosis factor-α converting enzyme is competitively inhibited by the binding of Necl-2 to integrin β_4. Abundant expression of Necl-2 delays the integrin β_4 cleavage, and down-regulation of Necl-2 has an opposite effect. This possibility is in agreement with our findings that overexpression of Necl-2 delayed the TPA-induced hemidesmosome disassembly, whereas knockdown of Necl-2 enhanced it. In addition, it is also important to investigate whether overexpression of other Necl family members gives the same effect on the TPA-induced hemidesmosome disassembly, as was observed in Necl-2-overexpressing cells.

The effect of Necl-2 overexpression in cultured human keratinocytes have been reported by Giangreco *et al.* (38). They showed that overexpression of Necl-2 led to the up-regulation of the calcium/calmodulin-associated Ser/Thr kinase, increased calcium-independent intercellular adhesion, and inhibition of both cell motility and *in vitro* wound healing. Although they did not mention data regarding the difference of the hemidesmosome structure between the wild-type and Necl-2-overexpressing keratinocytes, inhibition of cell motility observed by Necl-2 overexpression could be partly explained by our findings of the Necl-2-dependent inhibitory effect of hemidesmosome disassembly. Thus, our findings could be applicable to epithelial cells expressing and forming classical hemidesmosomes.

In many types of cancer cells, integrin $\alpha_6\beta_4$ is up-regulated and hemidesmosomes are disrupted, eventually causing an enhancement of cancer cell movement (22). Thus, hemidesmosome disassembly is thought to be a critical process for the initiation of tumor invasion and metastasis. Necl-2 was identified as a tumor suppressor in human non-small cell lung cancer cell line (5), and we previously showed that Necl-2 regulates the heregulin-induced signaling pathways of the ErbB3/ErbB2 heterodimer for cell movement and survival (14). Hemidesmosomes in tumor cells, in which Necl-2 is down-regulated, might be easily disassembled; therefore, stable cell-ECM adhesion is lost, and the cells are released from the basement membrane, leading to tumor cell invasion and metastasis. Our finding of the inhibitory effect of Necl-2 on hemidesmosome disassembly will explain another mechanism for the tumor suppressive role of Necl-2.

We previously showed that Necl-5, another Necl family member, physically and functionally interacts with integrin $\alpha_v\beta_3$ and PDGF receptor and enhances the formation of a leading edge structure, such as lamellipodia, peripheral ruffles, focal complexes, and focal adhesions, in response to PDGF (39–41). We also showed that Necl-5 enhanced the PDGF-induced growth of microtubules and attracted them near the plasma membrane of the leading edge of NIH3T3 cells in an integrin $\alpha_v\beta_3$-dependent manner (42). The function of Necl-2 described here is opposite to that of Necl-5, which is overexpressed in many human cancer cells (43–45). Although both molecules interacts in *cis* with their specific integrins and growth factor receptors, Necl-2 suppresses hemidesmosome disassembly, preventing cell detachment from the basement membrane, whereas Necl-5 enhances cell movement and survival, characteristics of the metastatic cancer cells (39, 40). In certain physiological and pathological conditions, such as embryonic development and cancer progression, cells lose their connection to neighboring cells or the basement membrane and become free, which increases the likelihood for migration and proliferation. This phenomenon is called epithelial-mesenchymal transition (46). Necl-2 is abundantly expressed in epithelial cells but is not expressed in fibroblasts, whereas Necl-5 is the opposite. Therefore, it is likely that down-regulation of Necl-2 and up-regulation of Necl-5 during epithelial-mesenchymal transition leads to an enhancement of cell movement.

Acknowledgments—We thank Drs. A. Sonnenberg and J. C. Norman for generous gifts of reagents.

REFERENCES

1. Takai, Y., Miyoshi, J., Ikeda, W., and Ogita, H. (2008) *Nat. Rev. Mol. Cell Biol.* **9,** 603–615
2. Fukami, T., Satoh, H., Fujita, E., Maruyama, T., Fukuhara, H., Kuramochi, M., Takamoto, S., Momoi, T., and Murakami, Y. (2002) *Gene* **295,** 7–12
3. Shingai, T., Ikeda, W., Kakunaga, S., Morimoto, K., Takekuni, K., Itoh, S., Satoh, K., Takeuchi, M., Imai, T., Monden, M., and Takai, Y. (2003) *J. Biol. Chem.* **278,** 35421–35427
4. Gomyo, H., Arai, Y., Tanigami, A., Murakami, Y., Hattori, M., Hosoda, F., Arai, K., Aikawa, Y., Tsuda, H., Hirohashi, S., Asakawa, S., Shimizu, N., Soeda, E., Sakaki, Y., and Ohki, M. (1999) *Genomics* **62,** 139–146
5. Kuramochi, M., Fukuhara, H., Nobukuni, T., Kanbe, T., Maruyama, T., Ghosh, H. P., Pletcher, M., Isomura, M., Onizuka, M., Kitamura, T., Sekiya, T., Reeves, R. H., and Murakami, Y. (2001) *Nat. Genet.* **27,** 427–430
6. Wakayama, T., Ohashi, K., Mizuno, K., and Iseki, S. (2001) *Mol. Reprod Dev.* **60,** 158–164
7. Urase, K., Soyama, A., Fujita, E., and Momoi, T. (2001) *Neuroreport* **12,** 3217–3221
8. Biederer, T., Sara, Y., Mozhayeva, M., Atasoy, D., Liu, X., Kavalali, E. T., and Südhof, T. C. (2002) *Science* **297,** 1525–1531
9. Masuda, M., Yageta, M., Fukuhara, H., Kuramochi, M., Maruyama, T., Nomoto, A., and Murakami, Y. (2002) *J. Biol. Chem.* **277,** 31014–31019
10. Galibert, L., Diemer, G. S., Liu, Z., Johnson, R. S., Smith, J. L., Walzer, T., Comeau, M. R., Rauch, C. T., Wolfson, M. F., Sorensen, R. A., Van der Vuurst de Vries, A. R., Branstetter, D. G., Koelling, R. M., Scholler, J., Fanslow, W. C., Baum, P. R., Derry, J. M., and Yan, W. (2005) *J. Biol. Chem.* **280,** 21955–21964
11. Yageta, M., Kuramochi, M., Masuda, M., Fukami, T., Fukuhara, H., Maruyama, T., Shibuya, M., and Murakami, Y. (2002) *Cancer Res.* **62,** 5129–5133
12. Fukuhara, H., Masuda, M., Yageta, M., Fukami, T., Kuramochi, M., Maruyama, T., Kitamura, T., Murakami, Y., and Masvuda, M. (2003) *Oncogene* **22,** 6160–6165
13. Kakunaga, S., Ikeda, W., Itoh, S., Deguchi-Tawarada, M., Ohtsuka, T.,

Mizoguchi, A., and Takai, Y. (2005) *J. Cell Sci.* **118,** 1267–1277
14. Kawano, S., Ikeda, W., Kishimoto, M., Ogita, H., and Takai, Y. (2009) *J. Biol. Chem.* **284,** 23793–23805
15. Vivanco, I., and Sawyers, C. L. (2002) *Nat. Rev. Cancer* **2,** 489–501
16. Wilhelmsen, K., Litjens, S. H., and Sonnenberg, A. (2006) *Mol. Cell Biol.* **26,** 2877–2886
17. Falcioni, R., Antonini, A., Nisticò, P., Di Stefano, S., Crescenzi, M., Natali, P. G., and Sacchi, A. (1997) *Exp. Cell Res.* **236,** 76–85
18. Gambaletta, D., Marchetti, A., Benedetti, L., Mercurio, A. M., Sacchi, A., and Falcioni, R. (2000) *J. Biol. Chem.* **275,** 10604–10610
19. Guo, W., Pylayeva, Y., Pepe, A., Yoshioka, T., Muller, W. J., Inghirami, G., and Giancotti, F. G. (2006) *Cell* **126,** 489–502
20. Kawano, S., Mizutani, K., Miyata, M., Ikeda, W., and Takai, Y. (2010) *Genes Cells* **15,** 995–1001
21. Borradori, L., and Sonnenberg, A. (1999) *J. Invest. Dermatol* **112,** 411–418
22. Mercurio, A. M., Rabinovitz, I., and Shaw, L. M. (2001) *Curr. Opin. Cell Biol.* **13,** 541–545
23. Ikeda, W., Kakunaga, S., Itoh, S., Shingai, T., Takekuni, K., Satoh, K., Inoue, Y., Hamaguchi, A., Morimoto, K., Takeuchi, M., Imai, T., and Takai, Y. (2003) *J. Biol. Chem.* **278,** 28167–28172
24. Honoré, S., Pichard, V., Penel, C., Rigot, V., Prévôt, C., Marvaldi, J., Briand, C., and Rognoni, J. B. (2000) *Histochem. Cell Biol.* **114,** 323–335
25. Schoenenberger, C. A., Zuk, A., Zinkl, G. M., Kendall, D., and Matlin, K. S. (1994) *J. Cell Sci.* **107,** 527–541
26. Lussier, C., Basora, N., Bouatrouss, Y., and Beaulieu, J. F. (2000) *Microsc. Res. Tech.* **51,** 169–178
27. Rabinovitz, I., Toker, A., and Mercurio, A. M. (1999) *J. Cell Biol.* **146,** 1147–1160
28. Fogel, A. I., Akins, M. R., Krupp, A. J., Stagi, M., Stein, V., and Biederer, T. (2007) *J. Neurosci.* **27,** 12516–12530
29. Underwood, R. A., Carter, W. G., Usui, M. L., and Olerud, J. E. (2009) *J. Histochem Cytochem.* **57,** 123–142
30. Kleinman, H. K., McGarvey, M. L., Liotta, L. A., Robey, P. G., Tryggvason, K., and Martin, G. R. (1982) *Biochemistry* **21,** 6188–6193
31. Kleinman, H. K., McGarvey, M. L., Hassell, J. R., Star, V. L., Cannon, F. B., Laurie, G. W., and Martin, G. R. (1986) *Biochemistry* **25,** 312–318
32. Buxbaum, J. D., Liu, K. N., Luo, Y., Slack, J. L., Stocking, K. L., Peschon, J. J., Johnson, R. S., Castner, B. J., Cerretti, D. P., and Black, R. A. (1998) *J. Biol. Chem.* **273,** 27765–27767
33. Rio, C., Buxbaum, J. D., Peschon, J. J., and Corfas, G. (2000) *J. Biol. Chem.* **275,** 10379–10387
34. Kim, D. Y., Ingano, L. A., and Kovacs, D. M. (2002) *J. Biol. Chem.* **277,** 49976–49981
35. Tanaka, Y., Irie, K., Hirota, T., Sakisaka, T., Nakanishi, H., and Takai, Y. (2002) *Biochem. Biophys. Res. Commun.* **299,** 472–478
36. Tanabe, Y., Kasahara, T., Momoi, T., and Fujita, E. (2008) *Neurosci. Lett.* **444,** 16–21
37. Pal-Ghosh, S., Blanco, T., Tadvalkar, G., Pajoohesh-Ganji, A., Parthasarathy, A., Zieske, J. D., and Stepp, M. A. (2011) *J. Cell Sci.* **124,** 2666–2675
38. Giangreco, A., Jensen, K. B., Takai, Y., Miyoshi, J., and Watt, F. M. (2009) *Development* **136,** 3505–3514
39. Minami, Y., Ikeda, W., Kajita, M., Fujito, T., Amano, H., Tamaru, Y., Kuramitsu, K., Sakamoto, Y., Monden, M., and Takai, Y. (2007) *J. Biol. Chem.* **282,** 18481–18496
40. Amano, H., Ikeda, W., Kawano, S., Kajita, M., Tamaru, Y., Inoue, N., Minami, Y., Yamada, A., and Takai, Y. (2008) *Genes Cells* **13,** 269–284
41. Nagamatsu, Y., Rikitake, Y., Takahashi, M., Deki, Y., Ikeda, W., Hirata, K., and Takai, Y. (2008) *J. Biol. Chem.* **283,** 14532–14541
42. Minami, A., Mizutani, K., Waseda, M., Kajita, M., Miyata, M., Ikeda, W., and Takai, Y. (2010) *Genes Cells* **15,** 1123–1135
43. Gromeier, M., Lachmann, S., Rosenfeld, M. R., Gutin, P. H., and Wimmer, E. (2000) *Proc. Natl. Acad. Sci. U.S.A.* **97,** 6803–6808
44. Masson, D., Jarry, A., Baury, B., Blanchardie, P., Laboisse, C., Lustenberger, P., and Denis, M. G. (2001) *Gut* **49,** 236–240
45. Sloan, K. E., Eustace, B. K., Stewart, J. K., Zehetmeier, C., Torella, C., Simeone, M., Roy, J. E., Unger, C., Louis, D. N., Ilag, L. L., and Jay, D. G. (2004) *BMC Cancer* **4,** 73
46. Gumbiner, B. M. (2005) *Nat. Rev. Mol. Cell Biol.* **6,** 622–634